Proceedings of 2005 5th IEEE Conference on Nanotechnology
Nagoya, Japan, July 2005

The Effect of Device Geometry on the Static and Dynamic Response of Carbon Nanotube Field Effect Transistors

M. Pourfath*, H. Kosina*, B.H. Cheong†, W.J. Park‡, and S. Selberherr*
*Institute for Microelectronics, TU Vienna, Gußhausstraße 27–29, A-1040 Wien, Austria
Phone: +43-1-58801/36014, Fax: +43-1-58801/36099, Email: Pourfath@iue.tuwien.ac.at
† Computational Science and Engineering Lab,‡ Materials and Devices Lab,
Samsung Advanced Institute of Technology, Suwon 440-600, Korea

***Abstract*— A numerical study of ohmic contact carbon nanotube field effect transistors is presented. The effect of the gate-source and gate-drain spacers on the static and dynamic response of the device was studied. Simulation results suggest that by appropriately selecting the gate-source and gate-drain spacers both the dynamic and static characteristics of the device are improved.**

***Index Terms*— carbon nanotube field effect transistors, ambipolar behavior, quasi static approximation.**

I. Introduction

Exceptional electronic and mechanical properties together with nanoscale diameter make carbon nanotubes (CNTs) candidates for nanoscale field effect transistors (FETs). While early devices have shown poor device characteristics, high performance devices were achieved recently [1–4]. In short devices (less than 100 nm) carrier transport through the device is nearly ballistic [3, 5]. We solved the coupled Poisson and Schrödinger equation system to study the static response of CNTFETs. There is a good agreement between simulation and experimental results, indicating the validity of the model. The Quasi Static Approximation (QSA) was used to investigate the dynamic response of these devices.

The contact between metal and CNT can be of Ohmic [5] or Schottky type [6]. In this work we focus on Ohmic contact CNTFETs which theoretically [7] and experimentally [3] show better performance than Schottky contact devices. In a p-type device with ohmic contacts holes see no barrier while the barrier height for electrons is $\mathrm{E_g}$. By changing the gate voltage the transmission coefficient of holes through the device is modulated and as a result the total current changes [5]. However, unwanted ambipolar behavior is observed, which limits the static characteristics of the device by reducing the $I_{\mathrm{on}}/I_{\mathrm{off}}$ ratio. We show that by appropriately selecting the gate-source and gate-drain spacers not only the ambipolar behavior and static characteristics, but also the dynamic characteristics of the device are improved. Therefore by careful geometry design the device characteristics can be well optimized.

II. Approach

In this section the models which were used to study the static and dynamic response of CNTFETs are explained. As will be shown at the end of this section we achieve a good agreement between simulation and experimental results.

A. Static Response

In order to account properly for ballistic transport we have solved the coupled Poisson and Schrödinger equations.

$$\frac{\partial^2 V}{\partial \rho^2}+\frac{1}{\rho}\frac{\partial V}{\partial \rho}+\frac{\partial^2 V}{\partial z^2}=-\frac{Q}{\epsilon} \tag{1}$$

$$-\frac{\hbar^2}{2\mathrm{m}^*}\frac{\partial^2 \Psi^{n,p}_{s,d}}{\partial z^2}+(U^{n,p}-E)\Psi^{n,p}_{s,d}=0 \tag{2}$$

We have considered a cylindrical symmetric structure, in which the gate surrounds the CNT, such that the Poisson equation (1) is restricted to two-dimensions. In (2) superscripts denote the type of the carriers. Subscripts denote the contacts, where s stands for the source contact and d for the drain contact. For example, Ψ^n_s is the wave function associated with electrons that have been injected from the source contact. The Schrödinger equation is solved on the surface of the tube, and is restricted to one-dimension because of cylindrical symmetry. All our calculations assume a CNT with 0.5 eV band gap, corresponding to a diameter of 1.7 nm [3].

The space charge density in (1) is calculated as:

$$Q=\frac{\mathrm{q}(p-n)\delta(\rho-\rho_{cnt})}{2\pi\rho} \tag{3}$$

where n and p are the total electron and hole concentrations per unit length. In (3) δ/ρ is the Dirac delta function in cylindrical coordinates, indicating that carriers were taken into account by means of a sheet charge distributed uniformly over the surface of the CNT [8]. Including the source and drain injection components, the total electron concentration in the CNT is calculated as:

$$n=\frac{4}{2\pi}\int f_s|\Psi^n_s|^2dk_s+\frac{4}{2\pi}\int f_d|\Psi^n_d|^2dk_d \tag{4}$$

where $f_{s,d}$ are equilibrium Fermi functions at the source and drain contacts, respectively. The total hole concentration in the CNT is calculated analogously.

The Landauer-Büttiker formula is used for calculating the current:

$$I^{n,p} = \frac{4\mathrm{q}}{\mathrm{h}} \int [f_s^{n,p}(E) - f_d^{n,p}(E)] TC^{n,p}(E) dE \qquad (5)$$

where $TC^{n,p}(E)$ are the transmission coefficients of electrons and holes through the device. The factor 4 in (4) and (5) stems from the twofold band and twofold spin degeneracy.

B. Dynamic Response

To study the dynamic behavior of CNTFETs, the QSA was used. Generally in this method device capacitances are given by the derivatives of the various charges with respect to the terminal voltages,

$$C_{ij} = \chi_{ij} \frac{\partial Q_i}{\partial V_j}\bigg|_{V_{k\neq j}=0} \qquad (6)$$

where the indices i, j, k represent terminals (gate, source or drain), and $\chi_{ij} = -1$ for $i \neq j$ and $\chi_{ij} = +1$ for $i = j$. The differentiation of these expressions is performed numerically over steady state charges [9]. This method is widely used for the analysis of conventional semiconductor devices, where the charge in the semiconductor device is partitioned into two parts indicating the contribution of the source and drain contacts [9, 10]. For example, the gate-source capacitance is calculated by

$$C_{sg} = \frac{\partial Q_{se}}{\partial V_{gs}} + \frac{\partial Q_{sq}}{\partial V_{gs}} = C_{se} + C_{sq} \qquad (7)$$

where Q_{se} is total charge charge on the source contact and Q_{sq} is the total charge on the tube injected from the source contact. As shown in (7) the total gate-source capacitance is split into two components, the first term indicates the electrostatic gate-source capacitance and the second term is usually referred to as quantum capacitance [11]. The capacitance matrix has a rank of 3, and due to quantum capacitances the matrix elements are not reciprocal ($C_{ij} \neq C_{ji}$). In this work we assumed that only the gate voltage changes, whereas the voltages of the other terminals are kept constant. Therfore, the capacitance matrix simplifies to three components, and an equivalent circuit as shown in Fig. 1 is achieved [12]. In Fig. 1, g_m is the differential transconductance calculated by

$$g_m = \frac{\partial I_{ds}}{\partial V_{gs}} \qquad (8)$$

Based on the equivalent circuit in Fig. 1, the cutoff frequency of the device can be derived as

$$f_T = \frac{g_m}{2\pi C_{sg}\sqrt{1 + 2\frac{C_{dg}}{C_{sg}}}} \qquad (9)$$

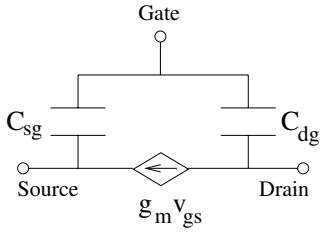

Fig. 1: Simplified equivalent circuit model for the dynamic response of CNTFETs. The model is based on the assumption that only the gate voltage changes.

C. Comparison with Experimental Data

For a fair comparison with experimental results, we used the same material and geometrical parameters as reported in [3]. As shown in Fig. 2, there is a good agreement between simulation and experimental results despite the fact that the cylindrical structure is only an approximation of the real device structure.

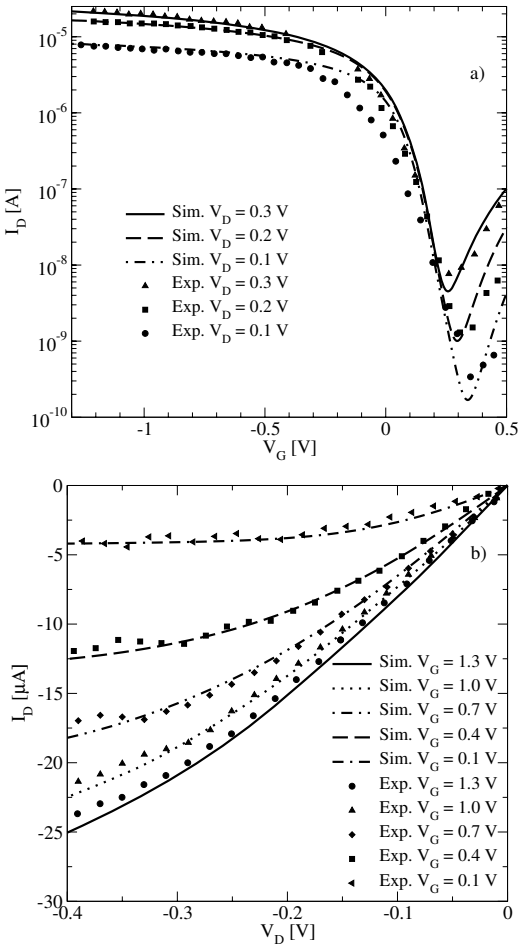

Fig. 2: Comparison of the experimental and simulation results a) Transfer characteristics, b) Output characteristics.

III. The Effect of Geometry on the Device Characteristics

First the operation of CNTFETs and the ambipolar behavior is explained. Then the effect of the gate-source and gate-drain spacers, L_S and L_D, (see Fig. 3) on the ambipolar behavior, static response, and dynamic response of CNTFETs is studied.

We consider a p-type ohmic device, similar to that reported in [3]. As shown in Fig. 2-a, the current has a minimum. This is the well known ambipolar behavior of these devices, which can be well understood by considering the band edge profiles of the device. As shown in Fig. 4, if the drain voltage becomes higher than the gate voltage, the barrier thickness for electrons at the drain contact is reduced and the tunneling current of electron increases. At the minimum point electrons and holes have the same contribution to the total current and in other regions either electrons or holes contribute mostly to the total current. This behavior is more apparent in Schottky contact devices, where both electrons and holes see a barrier height of $E_g/2$ [13]. We have shown that a double gate structure can be used to suppress the ambipolar behavior of Schottky contact devices [14]. In a double gate device the carrier injection at the source and drain contacts are controlled separately. In ohmic contact devices, however, because of asymmetric barrier heights even a single gate device can reduce the ambipolar behavior. As shown in Fig. 4, by increasing L_D the band edge profile near the drain contact is less affected by the gate voltage. Therfore, when the voltage between the gate and drain contacts increases the barrier thickness for electrons near the drain contact is less reduced, and as a result the tunneling current of electrons is suppressed. In Fig. 5 the transfer characteristics of devices with different L_D are presented. By increasing L_D the ambipolar behavior is suppressed, while the differential transconductance is not reduced. By suppressing the ambipolar behavior the I_{on}/I_{off} increases.

This method can not be applied to conventional MOSFETs. MOSFETs are charge controlled devices, by chang-

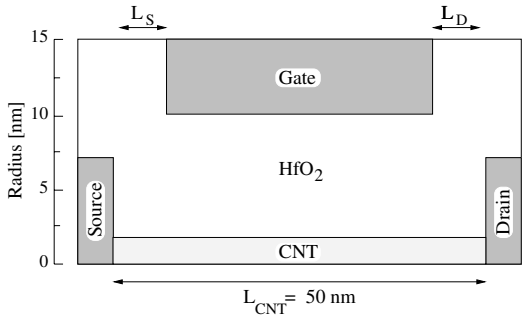

Fig. 3: Sketch of the cylindrical device.

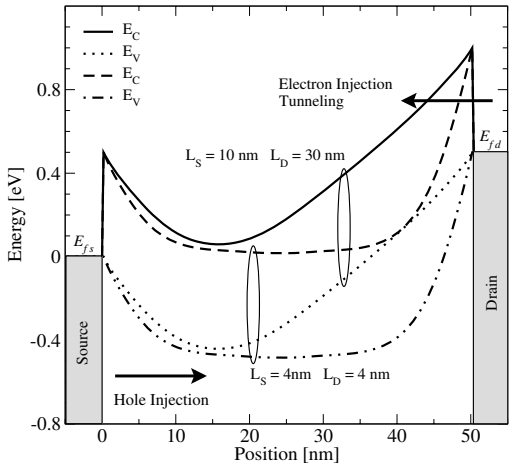

Fig. 4: The effect of L_S and L_D on the band-edge profiles of the device. $V_G = 0.5V$ and $V_D = -0.5V$.

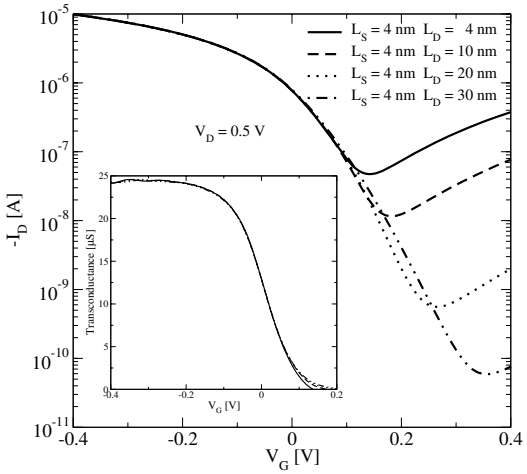

Fig. 5: The effect of L_D on the transfer characteristics of the device. The inset shows the differential transconductance.

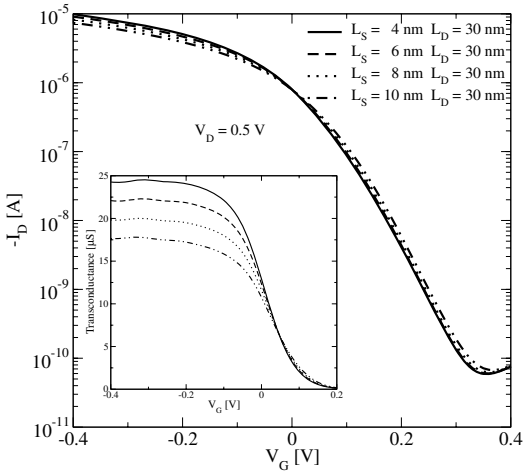

Fig. 6: The effect of L_S on the transfer characteristics of the device. The inset shows the differential transconductance.

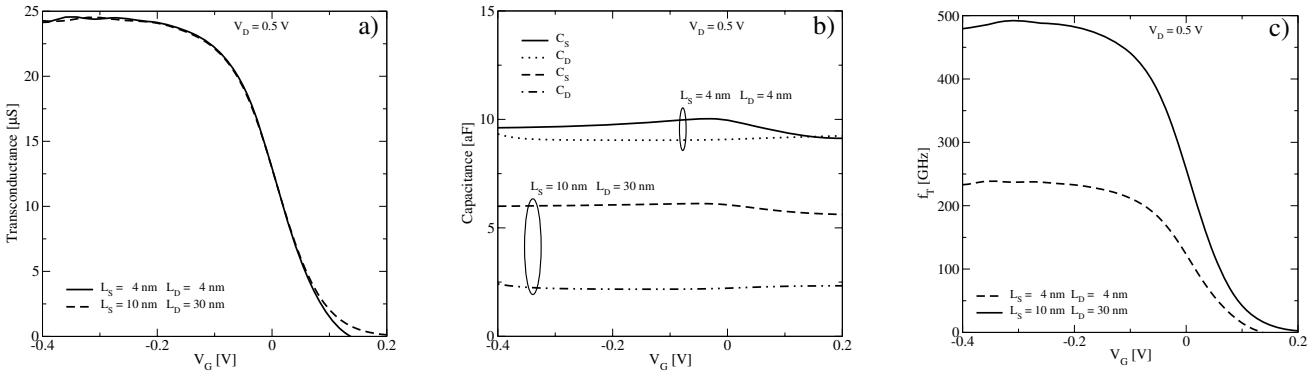

Fig. 7: a) Differential transconductance, b) Total capacitances, c) Cutoff frequencies of the devices with different L_S and L_D.

ing the gate voltage the channel conductivity is modulated. In contrast the channel of CNTFETs exhibits a constant conductivity ($G = 4q^2/h$ per mode) and the gate voltage modulates the transmission coefficient of carriers through the device. The band edge profile near the source contact plays an important role in determining the total current, since at high drain voltages all the carriers which cross the barrier near the source contact will be absorbed by the drain contact (neglecting minor quantum mechanical reflections).

In general, for a better frequency response the differential transconductance of a device should be increased and the parasitic capacitances should be decreased, see (9). We showed that by increasing L_D, the differential transconductance of the device is not affected, while the parasitic capacitance between gate and drain is reduced. By increasing L_S the parasitic capacitance between gate and source is reduced, and so is the differential transconductance, see Fig. 6. By appropriate selection of L_S and L_D optimization of the static and dynamic response of the device is possible. In Fig. 7-a and b the differential transconductance and the total gate-source and gate-drain capacitances for devices with different L_S and L_D are shown. The cutoff frequencies based on (9) are also shown in Fig. 7-c. The comparison of output characteristics and cutoff frequencies indicates that by increasing L_S and L_D both the static and dynamic response of the device are improved.

IV. Conclusion

We showed that for ohmic contact CNTFETs by appropriately selecting the gate-source and gate-drain spacers both the static and dynamic response of the device are improved. This method is not applicable to conventional MOSFETs because of different mechanisms in controlling the current flow through the device.

Acknowledgments

This work was partly supported by the European Commission, contract No. 506844 (NoE SINANO), and the National Program for Tera-level Nano-devices of the Korea Ministry of Science and Technology as one of the 21st Century Frontier Programs. Discussions with Prof. David Pulfrey are acknowledged.

References

[1] M. Radosavljevic, J. Appenzeller, P. Avouris, and J. Knoch, "High Performance of Potassium n-Doped Carbon Nanotube Field-Effect Transistors," *Appl.Phys.Lett.*, vol. 84, no. 18, pp. 3693–3695, 2004.

[2] B. M. Kim, T. Brintlinger, E. Cobas, H. Zheng, M. Fuhrer, Z.Yu, R. Droopad, J. Ramdani, and K. Eisenbeiser, "High-Performance Carbon Nanotube Transistors on SrTiO3/Si Substrates," *Appl.Phys.Lett.*, vol. 84, no. 11, pp. 1946–1948, 2004.

[3] A. Javey, J. Guo, D. B. Farmer, Q. Wang, E. Yenilmez, R. G. Gordon, M. Lundstrom, and H. Dai, "Self-Aligned Ballistic Molecular Transistors and Electrically Parallel Nanotube Arrays," *Nano Lett.*, vol. 4, no. 7, pp. 1319–1322, 2004.

[4] Y.-M. Lin, J. Appenzeller, J. Knoch, and P. Avouris, "High-Performance Carbon Nanotube Field-Effect Transistor with Tunable Polarities," *cond-mat/0501690*, 2005.

[5] A. Javey, J. Guo, Q. Wang, M. Lundstrom, and H. Dai, "Ballistic Carbon Nanotube Field-Effect Transistors," *Letters to Nature*, vol. 424, no. 6949, pp. 654–657, 2003.

[6] J. Appenzeller, M. Radosavljevic, J. Knoch, and P. Avouris, "Tunneling Versus Thermionic Emission in One-Dimensional Semiconductors," *Phys.Rev.Lett.*, vol. 92, p. 048301, 2004.

[7] J. Guo, S. Datta, and M. Lundstrom, "A Numerical Study of Scaling Issues for Schottky Barrier Carbon Nanotube Transistors," *IEEE Trans. Electron Devices*, vol. 51, no. 2, pp. 172–177, 2004.

[8] D. John, L. Castro, P. Pereira, and D. Pulfrey, "A Schrödinger-Poisson Solver for Modeling Carbon Nanotube FETs," in *Proc. NSTI Nanotech*, vol. 3, pp. 65–68, 2004.

[9] K.-M. Rho, K. Lee, M. Shur, and T. A. Fjeldly, "Unified Quasi-Static MOSFET Capacitance Model," *IEEE Trans. Electron Devices*, vol. 40, no. 1, pp. 131–136, 1993.

[10] S. E. Laux, "Techniques for Small-Signal Analysis of Semiconductor Devices," *IEEE Trans. Electron Devices*, vol. 32, no. 10, pp. 2028–2037, 1985.

[11] D. L. John, L. C. Castro, and D. L. Pulfrey, "Quantum Capacitance in Nanoscale Device Modeling," *J.Appl.Phys.*, vol. 96, no. 9, pp. 5180–5184, 2004.

[12] D. L. Pulfrey, L. Castro, D. John, M. Pourfath, A. Gehring, and H. Kosina, "Method for Predicting f_T for Carbon Nanotube Field-Effect Transistors," *submitted to IEEE Tran. Nanotechnology*, 2005.

[13] M. Radosavljevic, S. Heinze, J. Tersoff, and P. Avouris, "Drain Voltage Scaling in Carbon Nanotube Transistors," *Appl.Phys.Lett.*, vol. 83, no. 12, pp. 2435–2437, 2003.

[14] M. Pourfath, E. Ungersboeck, A. Gehring, B. H. Cheong, W. Park, H. Kosina, and S. Selberherr, "Improving the Ambipolar Behavior of Schottky Barrier Carbon Nanotube Field Effect Transistors," in *Proc. ESSDERC*, pp. 429–432, 2004.